

OPERATIONAL CHARACTERISTICS OF TUBE BENDS MADE USING LOCAL INDUCTION HEATING OF THE L360NE (X52) STEEL

The paper presents the evaluation of utility properties of a tube bend produced by bending process using local induction heating technique. Optimal process parameters were defined on the basis of numerical simulations. Mechanical testing procedures for the tube bend were carried out after normalising annealing. Heat treatment parameters have been chosen in compliance with the relevant standard. Geometrical measurements of the bend manufactured under industrial conditions indicate high accuracy of numerical simulations. Geometry and mechanical properties of the produced bend were consistent with the requirements of the applicable standards.

Keywords: L360NE (X52) steel, tube bending, computer simulation, mechanical properties

1. Introduction

Tube bends are used in construction of almost all pipelines. The development of bending processes has led to application of induction heating to heat the parts of the tube [1÷5]. When using this technique, called local induction heating, a narrow strip on the circumference of the tube (30÷50 mm) is heated when tube passes the induction heater during bending. Local induction heating enables the possibility of bending large diameter tubes (from 300 to 1600 mm) with relatively low values of bending radii. Using this technique during tube forming prevents fracturing, wall folding and deformations of cross section (Fig. 1).



Fig. 1. Incorrectly developed bends in the case of the bending being conducted with inappropriately chosen process parameters [6]

Bending with local induction heating was first used in the 1980s, and so it is a relatively new technology. Therefore it has

not been fully mastered and some aspects of it still lack complete explanation. Performance characteristics of tube bends depends on their geometry and mechanical properties [7,8]. While the geometry of the bend is shaped during bending with given process parameters (temperature, cooling rate etc.), the mechanical properties depend mainly on the parameters of heat treatment. Strength of tube bands should be as similar as possible to the strength of straight tube sections and geometric parameters of the tube (wall thickness and ovalisation) needs to conform with the standard [7].

2. Tube bending under industrial conditions

To obtain the optimal geometric of the bend (mainly a desired wall thickness in the tension-compression zone and a cross section ovalisation) relevant parameters of the bending process were chosen based on the results of numerical modelling [9,10]. In addition a heat treatment procedure was designed to ensure that the mechanical properties of the bend will comply with the standard [8,10].

Finite element method (FEM) numerical simulations were carried out using the Simufact Forming software packet. The model involved bending of tube made of L360NE (X52) steel about chemical composition: C-0,18; Mn-1,18; Si-0,19; P-0,005; Cu-0,04; Ni-0,03; Cr-0,19; Mo-0,008; V-0,033; Al-0,028.

The tube diameter was $\varnothing 323.9$ mm with the wall thickness of 8 mm and bending radius $R = 972$ mm. The deformability

* SILESIAAN UNIVERSITY OF TECHNOLOGY, INSTITUTE OF MATERIALS ENGINEERING, 8 KRASIŃSKIEGO STR., 40-019 KATOWICE, POLAND

** ZRE KATOWICE, 15 GEN. JANKEGO STR., 40-615 KATOWICE, POLAND

Corresponding author: grzegorz.junak@polsl.pl

of the used steel was assessed on the basis of plastometric hot compression tests (Fig. 2) carried out using the Gleeble 3800 simulator [11÷13].

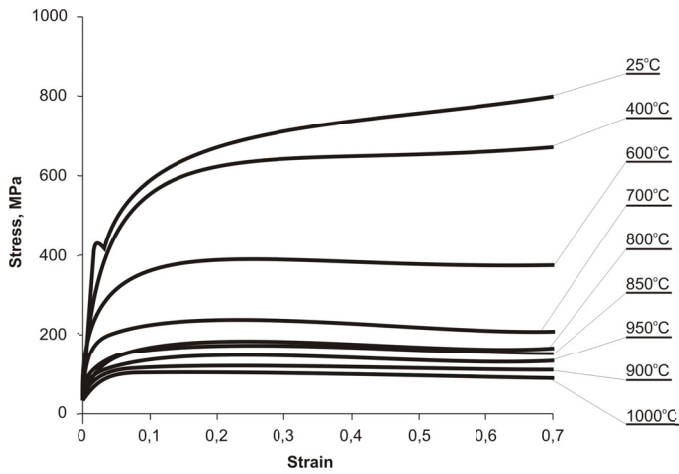


Fig. 2. Characteristics of deformability of steel grade L360NE (X52) on deformation rate of 0.1 s^{-1}

These characteristics showed that the flow stress values in given temperature are close to stable during deformation of the material in the temperature range from 400°C to 1000°C . The deformability characteristics of L360NE (X52) steel were used as material model in the numerical simulation of the bending process. During the calculations heating temperature value ranged from 800°C to 950°C and the tube pusher velocity was altered in the range between 30 mm/min and 55 mm/min . The model also included different cooling conditions of the tube bend after the bending zone: passive air cooling, cooling with forced air flow and water spray cooling (Tab. 1). Minimum cross section ovalisation value and the wall thickness in the tension-compression zone in compliance with the standard [9] were used as the optimisation criteria.

TABLE 1

Comparison of bending parameters for tubes made of the L360NE (X52) steel for selected variants of numerical simulations

Tube bend geometry	Modeling variant	Tube bending temperature, °C		Rate of travel, mm/min	Cooling method
		Compressed zone	Tensioned zone		
$R = 972 \text{ mm}$ $Dz = 323.9 \text{ mm}$ $g = 8 \text{ mm}$	I	820	850	30	Water spraying
	II	840	920	55	

An analysis of the results obtained from the calculations implied that, irrespective of the simulation variant, one could observe inhomogeneous intensity of plastic strain of the tube bend being formed – higher in the compressed zone and lower in the tensioned zone (Tab. 1). In the numerical calculations performed in accordance with the Cockcroft-Latham fracture criterion, the option of fractures occurring in the course of tube bending [13,14] was analysed by following dependence (1).

$$\int_0^\varphi \frac{\sigma_1}{\sigma_i} d\varphi \geq C_{gr} \tag{1}$$

where: σ_1 – the highest principal stress, σ_i – intensity of stress, φ – strain, C_{gr} – material constant established by experimental methods and considered as a required criterion

The aforementioned calculations evidenced that (Fig. 3), for the tube bending parameters assumed, the integral reached the value of ca. 0.2. The foregoing means that there is no hazard of the tube bend fracturing while bending, since the critical value of parameter C_3 on which the tube bend integrity may be compromised is $0.7 \div 1.0$.

The geometric features of a tube bend being formed, established by application of FEM, depending on the bending variant assumed, have been compared in Table 2. The geometric

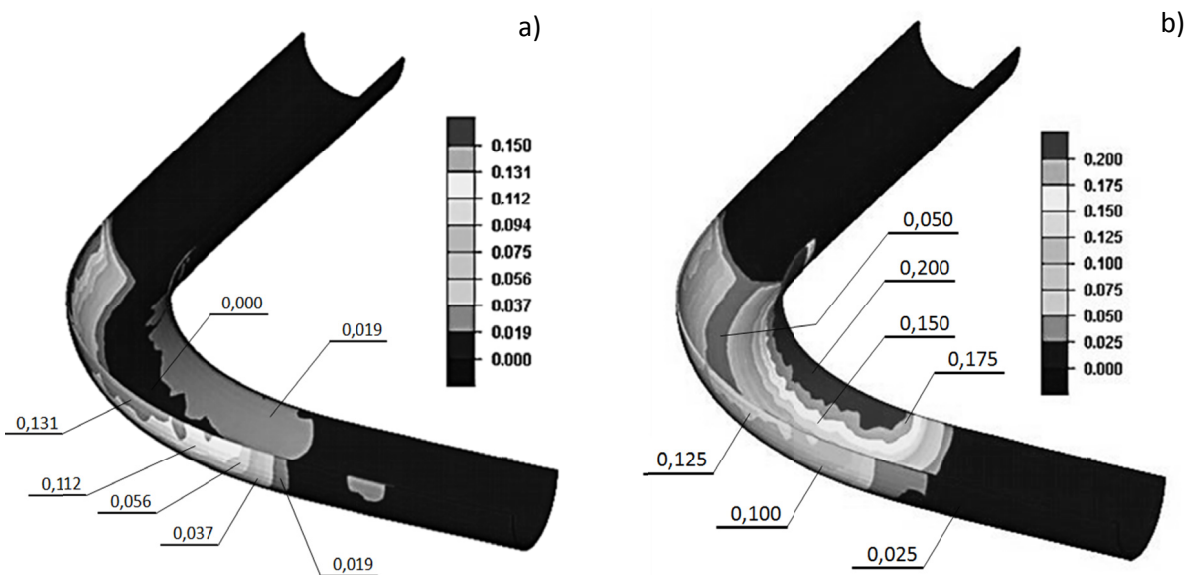


Fig. 3. Distribution of the Cockcroft-Latham fracture criterion (Fig. a) and deformation intensity values (Fig. b) on a tube bend cross section, as determined for bending variant I

features were measured in five cross sections, perpendicularly to the bending axis (Fig. 4).

Regardless of the calculation variant, one could find the wall thickness to increase by a similar value in the compressed zone of the bend and to decrease in the zone subject to tension. What the simulations also revealed was a considerable impact of the bending parameters on the bend cross section ovalisation. A bend formed on the parameters corresponding to variant I showed ovalisation of $e = 6.5\%$, i.e. lower than the value of $e_k = 6.67\%$ considered as a criterion in the applicable standard, which had been assumed as a threshold for industrial applications. On the other hand, bending simulation variant II displayed the bend ovalisation being higher than the permissible value.

The optimal bending process parameters obtained using numerical simulation were as follows: modelling variant I – heating temperature of 820/850°C and tube pusher velocity of 30 mm / min. Additionally the water spray method was chosen to cool the tube after the heating zone (Tab. 1).

TABLE 2

Bend geometric features established by FEM for selected modelling variants

Modelling variant	Mean wall thickness, mm		Mean tube cross section diameter, mm		Cross section ovalisation, % $e = \frac{2(D_a - D_b)}{D_a + D_b}$
	Compressed zone	Tensioned zone	D_b	D_a	
I	9.4	7.5	309.4	330.2	6.5
II	9.2	7.4	303.6	338.5	10.9
Standard requirements [6]	7.2	6.4	—	—	6.67

Bending process parameters determined by numerical simulation were used to manufacture the experimental tube bend using a bender depicted schematically in Fig. 5. Measurements of geometric features of the bend were compared to values obtained during simulation (Tab. 3).

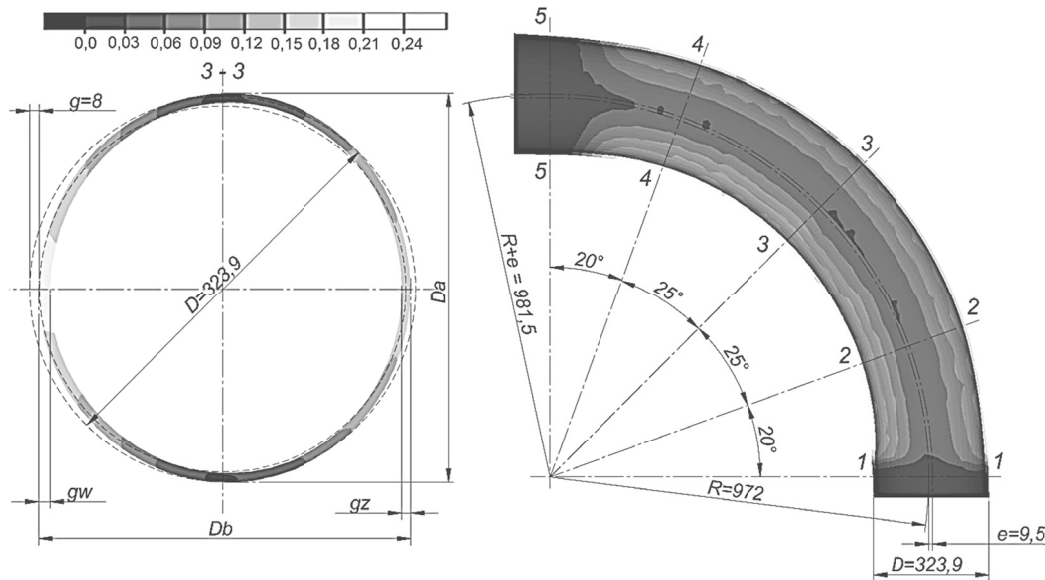


Fig. 4. Change of the tube cross section geometry in the bending zone determined by FEM

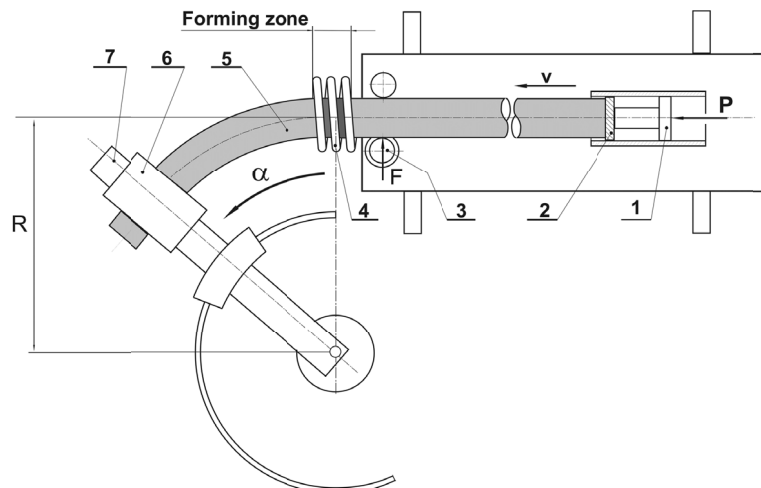


Fig. 5. Diagram of a tube bender with induction heating: 1 – Tube pusher, 2 – Clamping piece, 3 – Guiding rollers, 4 – Inductor, 5 – Tube being bent, 6 – Mechanism for the tube end clamping, 7 – Forming arm, P – pushing force

TABLE 3

Comparison of calculated, measured and required geometry of the tested tube bend

Promotion method	Tube wall thickness, mm		Tube diameter, mm		Cross section ovalisation, % $e = \frac{2(D_a - D_b)}{D_a + D_b}$
	Compression zone g_w	Tension zone g_z	D_b	D_a	
FEM simulation	9.4	7.5	309.4	330.2	6.5
Industrial trial	11.3	7.7	320.0	332.1	3.7
Standard requirements [9]	min. 7.2	min. 6.4	—	—	max. 6.7

The comparison indicate high accuracy of numerical simulation. Geometry of the manufactured bend was in compliance

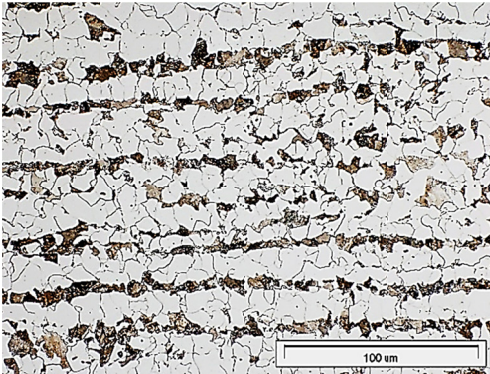
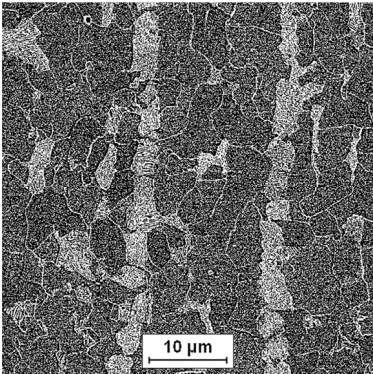
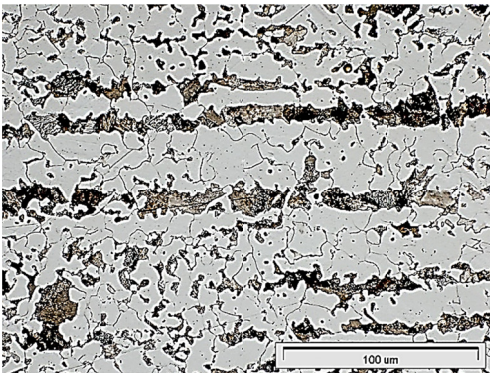
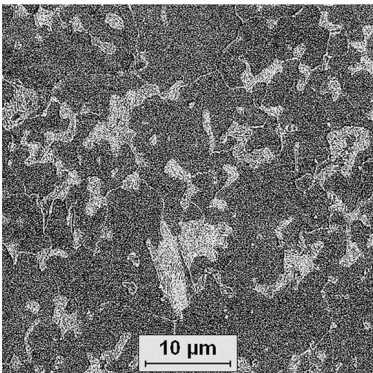
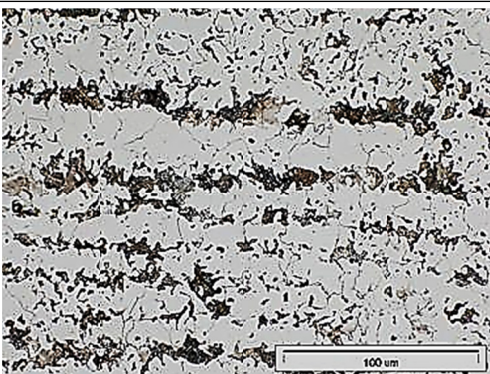
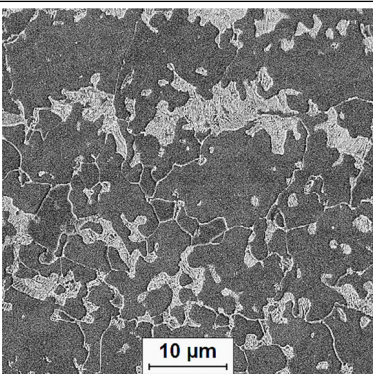
with the standard [9]. The bend was subjected to heat treatment in the form of normalising annealing with parameters as follows: 920°C/10 min with passive air cooling.

3. Material testing

Results of the static tension, hardness and impact tests were used to assess the mechanical properties of both, the tube and the manufactured experimental bend. Samples for testing purposes were taken from the tube in as-delivered state and from selected zones of the manufactured bend corresponding to tension and compression zones. The test specimens were cut out in accordance with the circumferential direction of the arc. The microstructure of the samples (Tab. 4) was analysed using optical microscope (OM), scanning electron microscope (SEM). Results of all tests have been presented in Tab. 5.

TABLE 4

Comparison of microstructures of the as-delivered tube and the bend made of the L360NE (X52) steel after normalisation heat treatment

Points of sampling for material testing		
	OM	SEM
as-delivered tube		
bend, tension zone		
bend, compression zone		

An analysis of the results obtained implies a drop in strength $UTS(R_m)$ by ca. 10% and in the value of parameter $YS(R_{t0.5})$ by ca. 30% for the tube bend material as compared with the as-delivered tube. Values of plastic properties of the tube bend material (A), on the other hand, increased compared to the as-delivered tube by ca. 30-50%. What could also be found was a drop in the tube HV10 hardness (by ca. 10%) on practically unaltered impact energy KV.

Optical microscopy analysis has revealed the banded, ferritic-pearlitic structure in the as-delivered tube and the samples of the manufactured bend as well.

The observed there grain was finer and the distance between the pearlite and ferrite bands was lower in the as-delivered samples than in ones from the tension, compression zones of the tube bend.

It is likely these features cause the mechanical properties significantly differ (Table 5). Material of the manufactured tube bend has lower strength $YS(R_{t0.5})$ and higher plastic (A) properties in comparison with as-delivered tube material.

TABLE 5

Comparison of mean values of basic mechanical properties of the L360NE (X52) steel tube samples at room temperature, according to Norm PN-EN-ISO 3183

Sampling point location	UTS(R_m), MPa	YS($R_{t0.5}$), MPa	A, %	KV, J	HV10
as-delivered tube	594	506	24	71	181
bend, tension zone	551	364	36	74	166
bend, compression zone	546	370	32	74	159
Standard [10]	460÷760	360÷530	—	min. 27	143÷193

4. Conclusions

The results of conducted tests show that the bending process and heat treatment parameters were chosen correctly, and that they ensured compliance with requirements of the applicable standards in terms of geometry as well as mechanical properties of a tube bend made of the L360NE (X52) steel.

It should also be noted that bending caused significant reduction in the tube bend strength properties considered as standard criteria, namely of parameter $YS(R_{t0.5})$ and strength $UTS(R_m)$. In order to obtain better strength properties of tube bends produced by the method addressed in this paper, the following actions

should be considered: modification of normalising annealing parameters (time and temperature) or replacing the normalising annealing with stress relief annealing aimed at eliminating the residual stresses emerging in the course of tube bending.

REFERENCES

- [1] Z. Hu, J.Q. Li, Computer simulation of pipe-bending processes with small bending radius using local induction heating. *Journal of Materials Processing Technology* **91**, 75-79 (1999).
- [2] M. Cieřła, R. Findziński, G. Junak, T. Kawała, The effect of heat treatment parameters on mechanical characteristics of 10CrMo9-10 steel tube bends, *Archives of Metallurgy and Materials* **60** (4), 2971-2976 (2015).
- [3] Z.T. Wang, Z. Hu, Theory of pipe-bending to a small bend radius using induction heating. *J. Mater. Process. Technology* **21** (3), 275-284 (1990).
- [4] M. Farzin, F. Ahmadi, Finite element simulation of induction bending of large diameter pipes with a small bending radius. *Journal of Steel research international* **1** (79), 179-185 (2008).
- [5] W. Kubiński, Hot production of tube bends, *Hutnik – Wiadomości Hutnicze* **12**, 467-471 (2001).
- [6] M. Cieřła, K. Mutwil, J. Tomczak, T. Kawała, Numerical Modeling as the Method to Determine the Parameters of Tube Bending with Local Induction Heating, *Solid State Phenomena* **246**, 313-216 (2016).
- [7] J. Pacanowski, Z. Kosowicz, Analysis of the influence of the tube bending method on the deformation of a tube bend, *Rudy i Metale Niezelazne* **10**, 419-423 (1996).
- [8] M. Cieřła, J. Tomczak, E. Hadasik, R. Findziński, T. Kawała, Performance characteristics of tubes made of X10CrMoVNb9-1 high temperature steel by bending process with zone-induction heating, *Hutnik-WH* **81** (7), 487-491 (2014).
- [9] PN EN 12952-5, Water-tube boilers and auxiliary installations Part 5.
- [10] PN-EN-ISO 3183 Petroleum and natural gas industries. Steel pipe for pipeline transportation systems.
- [11] E. Hadasik, I. Schindler, *Plasticity of metallic materials*, Publishers of the Silesian University of Technology, Gliwice (2004).
- [12] I. Schindler, et al., Activation energy in hot forming and recrystallization models for magnesium alloy AZ31, *Journal of Materials Engineering and Performance* **22** (3), 890-897 (2013).
- [13] P. Kawulok, et al., Credibility of various plastometric methods in simulation of hot rolling of the steel round bar, *Metalurgija* **53** (3), 299-302 (2014).